

Atomic layer deposition of lanthanum aluminum oxide nano-laminates for electrical applications

Booyong S. Lim, Antti Rahtu, Philippe de Rouffignac, and Roy G. Gordon

Department of Chemistry and Chemical Biology, Harvard University, Cambridge, Massachusetts 02138

(Received 26 September 2003; accepted 12 March 2004; published online 3 May 2004)

Lanthanum aluminum oxide thin films were grown by atomic layer deposition from a lanthanum precursor, tris(*N,N'*-diisopropylacetamidinato)lanthanum ($\text{La}(\text{PrAMD})_3$), trimethylaluminum and water. Smooth, amorphous films having compositions $\text{La}_{0.5}\text{Al}_{1.5}\text{O}_3$ and $\text{La}_{0.9}\text{Al}_{1.1}\text{O}_3$ were deposited on HF-last silicon and characterized without postdeposition annealing. The films contained less than 1 at. % of carbon according to Rutherford backscattering spectrometry and secondary ion mass spectrometry. A thin (9.8 nm) film showed low leakage current ($<5 \times 10^{-8}$ A/cm² at 1 V for an equivalent oxide thickness of 2.9 nm), flatband voltage of -0.1 V and low hysteresis (20 mV). Thicker films had even lower leakage currents ($<10^{-8}$ A/cm² at 2 MV/cm) but larger flatband shifts and more hysteresis. The permittivity of the films was 13 and the dielectric strength 4 MV/cm. Cross sectional high-resolution transmission electron microscopy showed a sharp interface between the film and the silicon substrate. © 2004 American Institute of Physics.

[DOI: 10.1063/1.1739272]

La_2O_3 is one of the most interesting high-*k* materials that could be used in metal-oxide-semiconductor field effect transistors (MOSFETs) and dynamic random access memories (DRAMs).¹ It has a high permittivity ($\epsilon_r=27$),² low leakage current due to a relatively large band gap ($E_g=5.8$ eV), high band offset with respect to silicon (>2 eV),^{3,4} and it should be thermodynamically stable in contact with silicon.⁵ La_2O_3 films have been grown using several physical and chemical deposition methods such as molecular beam epitaxy, evaporation, chemical vapor deposition (CVD), and atomic layer deposition (ALD). ALD is a very attractive method for depositing advanced gate oxides and DRAM insulators, because the film thickness is easy to control, and the uniformity across the wafer and deep trenches is better than with competing deposition methods. However, ALD of La_2O_3 has been a challenge. The only process realized so far used $\text{La}(\text{THD})_3$ and ozone.^{6,7} However, this process yields a relatively high carbon impurity content (~ 2 at. %), which might be detrimental for devices. Another drawback of the process is that ozone tends to oxidize the silicon surface during the deposition. Water would be a more attractive oxidizing agent because it should not oxidize the silicon surface below 300 °C.^{8,9} However, $\text{La}(\text{THD})_3$ is not reactive enough towards water to be used in ALD.

To overcome these problems we designed an ALD lanthanum precursor: tris(*N,N'*-diisopropylacetamidinato)lanthanum, $\text{La}(\text{PrAMD})_3$. The synthesis and properties of this compound have been described,¹⁰ and it is now commercially available.¹¹ It is the most volatile lanthanum compound known, subliming at 80 °C at a pressure of 0.04 Torr. Furthermore, it reacts rapidly with water, so it can be used for CVD and ALD of La_2O_3 . A problem of using water for ALD of lanthanum oxide is that the film reacts with water vapor to form lanthanum hydroxide.⁶ Lanthanum hydroxide then desorbs water continuously even after a long purge time and reacts with the next pulse of lanthanum precursor by a

CVD reaction, ruining the self-limited nature of the ALD reaction. To overcome this water adsorption/desorption problem we deposited alternating layers ($<a$ few nm thick) of La_2O_3 and Al_2O_3 to form a nanolaminate film. The aluminum oxide layers are impervious to water, limiting the water diffusion to only the thin La_2O_3 layer closest to the surface. Therefore the excess water in this thin La_2O_3 layer can be desorbed without using an excessively long purge time. ALD of aluminum oxide from trimethylaluminum (TMA) and water is a well-characterized process.^{12,13} It is currently used commercially in DRAM^{14,15} and hard drive read/write head applications.¹⁶

The films were deposited with a flow-type reactor operated at 0.3 Torr.¹⁷ The lanthanum precursor was kept at 130 °C and the TMA and water at room temperature. A saturating dose was used for all precursors. The growth temperatures were 300–330 °C. No self-decomposition of the lanthanum precursor was observed on substrates below 350 °C. The nanolaminate structure consisted of *m* cycles of lanthanum oxide growth and *n* cycles of aluminum oxide growth. This stack was repeated 4–25 times. The films were analyzed with ellipsometry, Rutherford backscattering spectrometry (RBS), secondary ion mass spectrometry (SIMS), atomic force microscopy, x-ray diffraction (XRD) and high-resolution transmission electron microscopy (HRTEM). The electrical properties were measured on *n*-type (5–10 Ω cm) silicon with an MDC 811 mercury probe. The area of the Hg contact was 4.2×10^{-3} cm². The La_2O_3 film grew as well on HF-last Si as it did on SiO_2 . The films for electrical measurements were grown on HF-last silicon in order to obtain the lowest effective oxide thickness (EOT). The leakage current was measured with a Keithley 2400 meter and the *C*–*V* curve with a HP 4275A meter.

Smooth (for 28 nm film, rms=1.2 nm) uniform films were obtained throughout the 25-cm-long deposition zone. With a 1:1 pulsing ratio the composition was $\text{La}_{0.5 \pm 0.1}\text{Al}_{1.5 \pm 0.1}\text{O}_3$, and with a 3:1 pulsing ratio the compo-

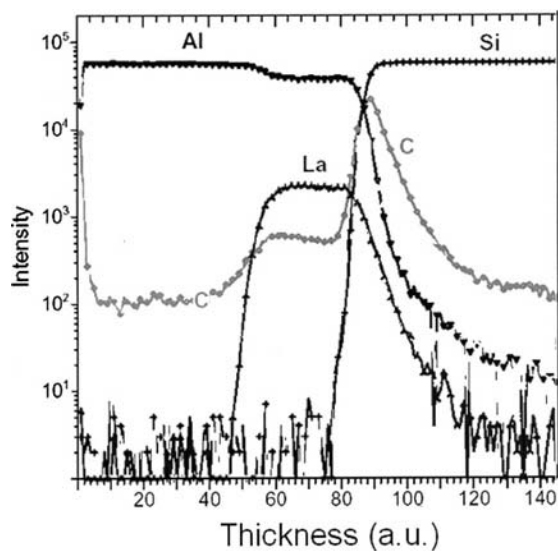


FIG. 1. The elemental depth profile measured by SIMS. The sample structure consists of: 250 cycles of $\text{Al}_2\text{O}_3/10^*$ (10 cycles of $\text{La}_2\text{O}_3 + 10$ cycles of Al_2O_3)/Si. The film was grown at 300°C . Note that the intensities do not reflect relative atomic ratios between different elements. Elevated carbon content at the surface and thin film/silicon interface may be due to non-clean room conditions in which the experiment was conducted.

sition was $\text{La}_{0.9\pm 0.1}\text{Al}_{1.1\pm 0.1}\text{O}_3$. The total metal to oxygen ratio was 2:3 in all films. The $\text{La}_{0.5}\text{Al}_{1.5}\text{O}_3$ films had a refractive index of 1.73. The refractive index increased to 1.8 for the $\text{La}_{0.9}\text{Al}_{1.1}\text{O}_3$ films. These values are reasonable for a nanolaminate containing Al_2O_3 ($n=1.64$) and La_2O_3 ($n=2$). For films grown at 330°C in which the nanolaminate was composed of 25 bilayers of first 10 cycles of La_2O_3 and then 10 cycles of Al_2O_3 , the thickness was 460 \AA . Each cycle consists of a metal precursor pulse and a water pulse with appropriate purge times to achieve a constant and self-limited growth rate. By using the known growth rate of Al_2O_3 from TMA and water, which is about 1.07 \AA/cycle , the growth rate of La_2O_3 can be estimated to be 0.8 \AA/cycle .

The films were pure according to RBS. To get a more sensitive estimate of its purity, a film was analyzed with SIMS (Fig. 1). SIMS is a very sensitive analysis tool, however, it is difficult to quantify results because the sensitivity is subject to matrix effects and standards are not available for carbon in metal oxides. To overcome this problem, we deposited a pure Al_2O_3 film on top of a nanolaminate structure. ALD from TMA and water at 300°C is known to produce very pure Al_2O_3 , with carbon levels less than 0.2%, the detection limit of the time of flight-elastic recoil detection analysis (TOF-ERDA) method.¹⁸ The carbon content in the nanolaminate is about five times higher than the carbon content in the Al_2O_3 , and is thus less than about 1%. The film was not exposed to air between the nanolaminate and Al_2O_3 growth. The hydrogen level in the SIMS (not shown) was the same for the Al_2O_3 and for the nanolaminate structure. According to the TOF-ERDA analysis, this hydrogen level should be about 0.7%.¹⁹ This low level of hydrogen should not introduce significant amounts of mobile or fixed charge. Lithium and chlorine were also observed in the SIMS (not shown). However, these impurities are traces left from the precursor synthesis; they can be avoided by more careful purification of the precursor.

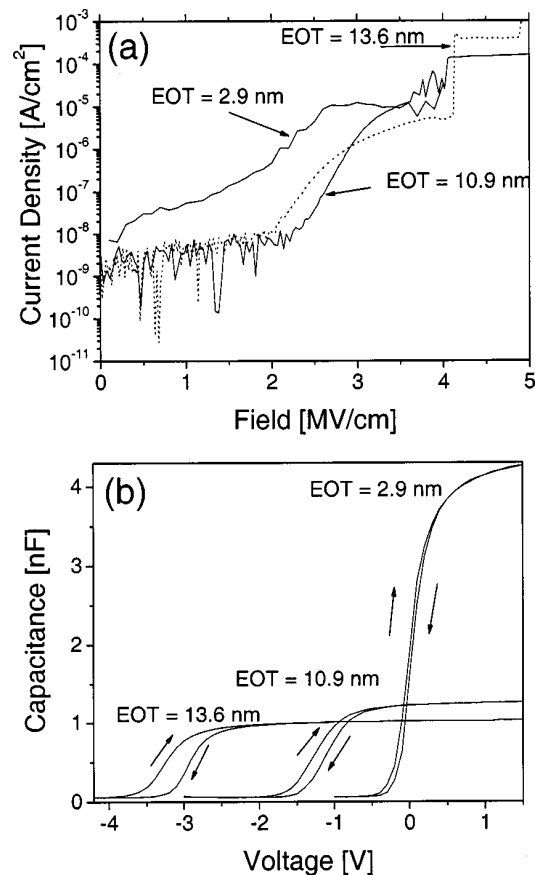


FIG. 2. (a) The I - V and (b) C - V curves for lanthanum aluminum oxide films. The optical thicknesses were 9.8 nm of $\text{La}_{0.9}\text{Al}_{1.1}\text{O}_3$ (EOT = 2.9 nm), 28 nm of $\text{La}_{0.5}\text{Al}_{1.5}\text{O}_3$, (EOT=10.9 nm) and 46 nm of $\text{La}_{0.5}\text{Al}_{1.5}\text{O}_3$ (EOT=13.6 nm). The measurement frequency was 100 kHz.

Figure 2(a) shows the leakage current as a function of voltage. For the 9.8-nm-thick film the leakage current at 1 V is $5 \times 10^{-8} \text{ A/cm}^2$ [Fig. 2(a)]. This film having an equivalent oxide thickness (EOT) of 2.9 nm meets the leakage current requirements for DRAM.²⁰ For the 28- and 46-nm-thick films the leakage current stayed below 10^{-8} A/cm^2 up to 2 MV/cm. The breakdown field was 4 MV/cm. Figure 2(b) shows C - V curves for the same spots as the I - V curves shown in Fig. 2(a). The permittivity of this nanolaminate is 13. By assuming linear scaling from pure Al_2O_3 ($\epsilon_r \sim 9$) to La_2O_3 ($\epsilon_r \sim 27$) with the composition of $\text{La}_{0.5}\text{Al}_{1.5}\text{O}_3$ the permittivity should be 13.5. These values are in good agreement.

For a 9.8-nm-thick film (EOT=2.9), the C - V curve shown in Fig. 2(b) shows that the flatband voltage is around zero and that the capacitor has fully inverted at -1 V . The hysteresis is only 20 mV for the as-deposited film. Curves were fitted using the Hauser simulation program and showed behavior similar to ideal C - V curves.²¹

The two thicker films in Fig. 2(b) show large negative flatband shifts, indicating positive trapped charge. Oxide films with trapped charges tend to show V_{FB} shifts increasing with thickness. Because of the nanolaminate nature of these films, increasing thickness also increases the number of oxide/oxide interfaces, which can also lead to a net increase in trapped charge.²² A large negative shift is usually seen for lanthanum oxide films.²³ Aluminum oxide usually causes a

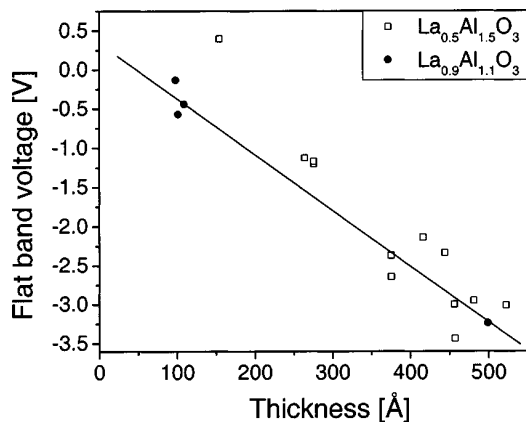


FIG. 3. Flatband voltage as a function of thickness for nanolaminate lanthanum aluminum oxide films starting with La_2O_3 . The ideal V_{FB} expected for this measurement is $+0.17$ V. The line is fit to the points (filled circles) for nanolaminates with composition $\text{La}_{0.9}\text{Al}_{1.1}\text{O}_3$, giving an intercept of 0.3 V, just slightly higher than the ideal value 0.17 V. The points (squares) for the composition $\text{La}_{0.5}\text{Al}_{1.5}\text{O}_3$ correspond to a more positive flatband shift.

positive shift because of aluminum centers which are known to trap negative charge.²⁴ The material first in contact with silicon was found to have an important effect on the flatband voltage. If aluminum was the first layer, a positive shift ($V_{\text{FB}} = +0.6$ V) was observed. It seems that lanthanum oxide is a better starting layer than aluminum oxide because thin films in which lanthanum oxide was the first layer had nearly zero flatband shift (Fig. 3). By adjusting the lanthanum to aluminum ratio and the thickness of the nanolaminates, the flatband shift can be adjusted to zero or even a slightly positive value.

The hysteresis for a 46-nm-thick film was rather large, 290 mV. For thinner films both the flatband voltage shift and hysteresis were reduced. For a 28-nm-thick film the flatband shift was -1.2 V and the hysteresis was reduced to 145 mV [Fig. 2(b)]. Hysteresis, seen as a positive ΔV_{FB} , is indicative of negative charge injection into the film from the gate or the substrate. The permittivity for the thin films was 13, and it

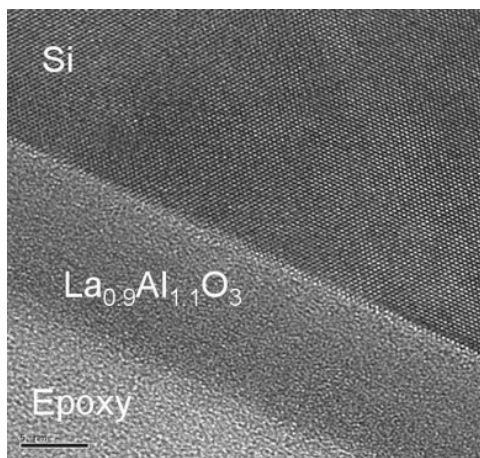


FIG. 4. Cross sectional TEM images of 9.8-nm thick lanthanum aluminum oxide film grown on HF-last silicon with a pulsing ratio of 16 La : 6 Al. The scale bar is 5 nm.

decreased only 3% when the measurement frequency was increased from 10 to 400 kHz.

Figure 4 shows a HRTEM image of a film (EOT of 2.9 nm) grown on HF-last silicon. It can be seen that the film was amorphous and the Si-film interface contained no interfacial layer. This was supported by other XRD data in which no peaks were observed. From a separate low-resolution TEM it was seen that the film was smooth and well nucleated across the silicon surface.

In conclusion, smooth, amorphous, and uniform lanthanum aluminum oxide films with an EOT of 2.9 nm were deposited by ALD. As-deposited thin films had low leakage current ($<5 \times 10^{-8}$ A/cm² at 1 MV/cm). Thin films had small flatband shifts and small hysteresis (20 mV). The breakdown field was 4 MV/cm. The films grew uniformly on HF-last silicon with very thin, if any, interfacial layers.

The authors thank Dr. Martin Gutsche at Infineon for SIMS analysis and Mr. Cheng-Yen Wen for TEM images. This work was supported in part by the National Science Foundation.

- ¹A. I. Kingon, J.-P. Maria, and S. K. Streiffer, *Nature (London)* **406**, 1032 (2000).
- ²Y. H. Wu, M. Y. Yang, A. Chin, W. J. Chen, and C. M. Kwei, *IEEE Electron Device Lett.* **21**, 341 (2000).
- ³J. Robertson, *Appl. Surf. Sci.* **190**, 2 (2002).
- ⁴P. W. Peacock and J. Robertson, *J. Appl. Phys.* **92**, 4712 (2002).
- ⁵K. J. Hubbard and D. G. Schlom, *J. Mater. Res.* **11**, 2757 (1996).
- ⁶M. Nieminen, M. Putkonen, and L. Niinistö, *Appl. Surf. Sci.* **174**, 155 (2001).
- ⁷M. Nieminen, T. Sajavaara, E. Rauhala, M. Putkonen, and L. Niinistö, *J. Mater. Chem.* **11**, 2340 (2001).
- ⁸M. M. Frank, Y. J. Chabal, and G. D. Wilk, *Appl. Phys. Lett.* **82**, 4758 (2003).
- ⁹Y. B. Kim, M. Tuominen, I. Raaijmakers, R. de Blank, R. Wilhelm, and S. Haukka, *Electrochem. Solid-State Lett.* **3**, 346 (2000).
- ¹⁰B. S. Lim, A. Rahtu, J. S. Park, and R. G. Gordon, *Inorg. Chem.* **42**, 7951 (2003).
- ¹¹Private communication from Dr. Marek Boleslawski, mboleslawski@sial.com at the Sigma-Aldrich Chemical Company.
- ¹²L. G. Gosset, J.-F. Damlencourt, O. Renault, D. Rouchon, Ph. Holliger, A. Ermolieff, I. Trimaille, J.-J. Ganem, F. Martin, and M.-N. Semeria, *J. Non-Cryst. Solids* **303**, 17 (2002).
- ¹³R. Matero, A. Rahtu, M. Ritala, M. Leskelä, and T. Sajavaara, *Thin Solid Films* **368**, 1 (2000).
- ¹⁴J.-H. Lee, J. P. Kim, J.-H. Lee, Y.-S. Kim, H.-S. Jung, N.-I. Lee, H.-K. Kang, K.-P. Suh, M.-M. Jeong, K.-T. Hyun, H.-S. Baik, Y. S. Chung, X. Liu, S. Ramanathan, T. Seidel, J. Winkler, A. Londergan, H. Y. Kim, J. M. Ha, and N. K. Lee, *Tech. Dig.—Int. Electron Devices Meet.* **2002**, 221.
- ¹⁵T. Seidel, X. Liu, A. Londergan, A. Srivastava, E. Lee, and S. Ramanathan, *American Vacuum Society Topical Conference on Atomic Layer Deposition* (2003).
- ¹⁶M. Kautzky, R. Lambertson, S. Chakravarty, L. Stearns, A. Kumar, and J. Dolejsi, in Ref. 15.
- ¹⁷J. S. Becker and R. G. Gordon, *Appl. Phys. Lett.* **82**, 2239 (2003).
- ¹⁸R. Matero, A. Rahtu, M. Ritala, M. Leskelä, and T. Sajavaara, *Thin Solid Films* **368**, 1 (2000).
- ¹⁹R. Matero, PhD thesis, University of Helsinki, 2004.
- ²⁰H. Reisinger and R. Stengl, *IEEE D*, 26-1 (2000).
- ²¹J. R. Hauser and K. Ahmed, in *Characterization and Metrology for ULSI Technology*, edited by Seiler (AIP, New York, 1998), pp. 235–239.
- ²²D. Schroder, *Semiconductor Material and Device Characterization*, (Wiley, New York, 1998), pp. 337–419.
- ²³S. Guha, E. Cartier, M. A. Gribelyk, N. A. Bojarczuk, and M. C. Copel, *Appl. Phys. Lett.* **77**, 2710 (2000).
- ²⁴J. H. Lee, K. Koh, N. I. Lee, M. H. Cho, Y. K. Kim, J. S. Jeon, K. H. Cho, H. S. Shin, M. H. Kim, K. Fujihara, H. K. Kang, and J. T. Moon, *Tech. Dig.—Int. Electron Devices Meet.* **2000**, 645.